PLISKA
STUDIA MATHEMATICA

ПЛИСКА
МАТЕМАТИЧЕСКИ
СТУДИИ

Pliska Stud. Math. **25** (2015), 111–118

PLISKA
STUDIA MATHEMATICA

HEAT TRANSFER ANALYSIS FROM AN ELLIPTIC CYLINDER AT MODERATELY HIGH REYNOLDS NUMBER FLOWS

Yoshihiro Mochimaru, Daisuke Akita

Heat transfer from an elliptic cylinder placed normal to a uniform flow at moderately high Reynolds numbers is analyzed, using a spectral finite difference scheme. The subcritical field near the cylinder is assumed to be governed by a laminar potential flow with parametric variables. Not only a uniform surface temperature condition (Dirichlet type) but uniform heat flux condition (Neumann type) can be supported to show good agreement with traditional experimental data.

1. Introduction

Heat transfer from external surface due to cross flow is a typical element of compact heat exchangers. Thus, many reports have been presented, e.g. by Kakaç et al. [11] and Kakaç et.al. [10]. Experimental heat transfer from pin arrays (circular or elliptical) was reported, e.g. by Ciha [4], Lawson [13], and Saboya [16]. Experimental one from diamond-shaped fin array was reported by Hirasawa, Fijiwara, Kawanami, and Shirai [9], and one from a single finite finned type was reported by Ota, Aiba, Tsuruta, and Kaga [14] and Ventola, Chiavazzo, Calignano, Manfredi, and Asinari [17]. Experimental evaluation for compact heat exchanger type was reported, e.g. by Fehle, Klas, and Mayinger [6], and Riddell [15]. Under the circumstance of traditional heat exchangers (except micro heat exchangers) ambient fluid flow speed is relatively high but subcritical, and detailed information on velocity field throughout the field was hard to be obtained analytically or numerically, so that analytical treatment was limited. For example, Khan, Culham, and Yovanovich [12] gave an analysis based on

2010 *Mathematics Subject Classification:* 35C10, 35Q30, 65N06, 76D05, 76R05, 80M22
Key words: Heat Transfer, High Reynolds number, Spectral Analysis, Finite Difference

boundary-layer approximation using finite order polynomial; Allen and Look [2] & Frick and McCullough [7] gave approximate analysis using Reynolds analogy (at least assuming Prandtl number = 1). For not so high Reynolds number, Zhang and Balachandar [18] presented results using finite difference scheme (staggered grids) for compact heat exchangers, and Bhoite1, Gavhane, Gore, and Kanjvane [3] provided results using FEM for various fin types.

In this report heat transfer from an elliptic cylinder placed normal to a substantially uniform flow, the direction of which is parallel to its major axis, is analyzed assuming that the ambient fluid flow field is approximated by a potential flow.

2. Analysis

2.1. Basic equations

Steady-state heat and flow field is analyzed under subcritical (substantially incompressible) laminar conditions of Newtonian fluid. Fluid properties such as density, viscosity, and thermal conductivity are assumed to be independent of temperature. Far away ambient fluid flow and thermal conditions are assumed uniform. Then under a boundary fitted conformal coordinate system, the governing equations (equation of vorticity transport and the energy equation, neglecting dissipation terms) can be written, if for the Cartesian coordinate (x, y), $z \equiv x+iy$ is an analytic function of $\alpha + i\beta(\alpha, \beta : \text{real})$, as

$$\frac{\partial(\zeta, \psi)}{\partial(\alpha, \beta)} = \frac{1}{Re}\left(\frac{\partial^2}{\partial\alpha^2} + \frac{\partial^2}{\partial\beta^2}\right)\zeta, \tag{1}$$

$$J\zeta + \left(\frac{\partial^2}{\partial\alpha^2} + \frac{\partial^2}{\partial\beta^2}\right)\psi = 0, \tag{2}$$

$$\frac{\partial(T, \psi)}{\partial(\alpha, \beta)} = \frac{1}{Pr\ Re}\left(\frac{\partial^2}{\partial\alpha^2} + \frac{\partial^2}{\partial\beta^2}\right)T, \tag{3}$$

where ζ, ψ, T are dimensionless vorticity based on U_∞/a, stream function based on $U_\infty a$, and temperature defined as $T \equiv (\text{local temperature} - T_\infty)/\Delta$ respectively. U_∞, a, T_∞, Δ stand for far away uniform fluid speed, length of the semi-major axis of the cylinder, far away uniform fluid temperature, and reference temperature difference defined separately, respectively. The boundary fitted coordinate (dimensionless, based on a), is

$$x + i\,y \equiv z = \cosh(\alpha_0 + \alpha + i\,\beta)/\cosh\alpha_0 (0 \le \alpha \le \alpha_\infty), \alpha_0 \equiv \tanh^{-1}(b/a),$$

where b : the semi-minor axis , and $J \equiv |dz/d(\alpha + i\,\beta)|^2$. $\alpha = 0$ corresponds to the elliptic surface. Re is a Reynolds number based on the semi-major axis, a,

along the direction of which the free stream flows, and Pr stands for a Prandtl number. As long as a typical temperature difference in the field is not large, fluid properties can be considered to be constant, and the equation of vorticity transport and that of energy are uncoupled, if any thermal boundary conditions are independent of dynamic flow conditions, which applies to subcritical flows. If $Re \gg 1$, the flow just outside the cylinder can be governed [1] by a potential flow function, F,

$$F = \frac{\mathrm{e}^{\alpha_0}}{2\cosh\alpha_0}\left[2\cosh(\alpha + i\,\beta) + \frac{1}{1 - \sum_{n\geq 2}\epsilon_n \cosh n(\alpha + i\beta)} - 1\right]. \tag{4}$$

2.2. Reference temperature difference

In case of heated uniform surface temperature, $\Delta \equiv$ surface temperature $- T_\infty$. In case of emitting uniform heat flux, Q, $\Delta \equiv Q\,a/\kappa$, where κ: thermal conductivity.

2.3. Boundary conditions

Dynamic boundary conditions: no slip flow at the surface gives $\psi(\alpha = 0, \beta) = \partial\psi/\partial\alpha(\alpha = 0, \beta) = 0$. Far away conditions at $\alpha = \alpha_\infty$: $\dfrac{\partial\psi}{\partial\alpha}(\alpha = \alpha_\infty, \beta) = \Im\left(\dfrac{dF}{d\alpha}\right)_{\alpha=0}$, or equivalently $\psi(\alpha_\infty, \beta) = \Im F(\alpha_\infty + i\beta)$ as $Re \to +\infty$. For vorticity $\zeta(\alpha_\infty, \beta) = 0$. [$(\partial/\partial\alpha)\zeta(\alpha_\infty, \beta) = 0$: necessary condition.] Since for fluids except liquid metals, Prandtl number, Pr, is usually greater than 0.6, thermal boundary conditions: $T(\alpha_\infty, \beta) = 0$, and either for heated uniform temperature $T(\alpha = 0, \beta) = 1$ or for emitting uniform heat flux $\dfrac{1}{\sqrt{J}}\dfrac{\partial T}{\partial\alpha}(\alpha = 0, \beta) = -1$.

2.4. Spectral decomposition

Considering the symmetricity of the field, the following applies:

$$\begin{bmatrix} \zeta \\ \psi \end{bmatrix} = \sum_{n=1}^{\infty} \begin{bmatrix} \zeta_n(\alpha) \\ \psi_n(\alpha) \end{bmatrix} \sin n\beta, \quad T = \sum_{n=0}^{\infty} T_n(\alpha)\cos n\beta. \tag{5}$$

2.5. Local and mean Nusselt number

In case of uniform temperature, local Nusselt number, i.e. dimensionless local heat flux, Nu, based on the length a, is $Nu = -\dfrac{1}{\sqrt{J}}\dfrac{\partial T}{\partial\alpha}(\alpha = 0, \beta)$ and mean

Nusselt number, Nu_m, is $Nu_m \equiv \dfrac{1}{L_s}\oint Nu\sqrt{J}\,d\beta = -\dfrac{1}{L_s}\oint \dfrac{\partial T}{\partial \alpha}\,d\beta$, where L_s is a circumference length and $L_s \equiv \oint \sqrt{J}\,d\beta = 4\,\mathrm{E}\left(\dfrac{1}{\cosh\alpha_0}\right)$, where E() is a complete elliptic integral of the second kind. In case of uniform heat flux, local Nusselt number, Nu, is $Nu = 1/T\,(\alpha = 0, \beta)$ and mean Nusselt number, Nu_m (not the mean value of Nu), based on the mean surface temperature, T_m, is $Nu_m \equiv 1/T_m, \quad T_m \equiv \dfrac{1}{L_s}\oint \sqrt{J}\,T\,d\beta$.

2.6. Solution procedure

The governing equations are decomposed exactly into Fourier components. After separating the variable β through Eqs (1)–(3) in addition to boundary conditions, the system of equations is discretized in space α using finite difference approximation. Then by time marching method (supplying unsteady terms), first the system of vorticity transport can be solved (by truncating up to a certain order of Fourier component) to get a steady state solution as in [1]. Then the energy equation can be solved, truncating up to the same order, since the equation itself is linear in T. In these cases $\alpha_\infty \equiv \dfrac{5\,c}{\sqrt{Re}}$, where c is a suitable constant such that $c > 1$.

3. Results and discussions

3.1. Comparison of current results with experimental ones for an elliptic cylinder of $b/a = 1/2$

In general, at a separation point $dF/dz = 0$. In case of $0 \geq \epsilon_2 \geq -0.5, \epsilon_n (n \geq 3)$, no separation of flow on the elliptic cylinder is expected due to Eq. (4), since $|dF/dz|_{\alpha=0} \neq 0$, otherwise for a given combination of ϵ's $|dF/dz|$ may be equal to zero at some β or β's $(0 < \beta < \pi)$, the maximum of which corresponds to a separation point. Figure 1 shows local Nusselt number distribution for uniform surface temperature along the arc.

3.2. Comparison of computed heat transfer from an elliptic cylinder with experimental ones from a streamline body

Figure 2 shows local Nusselt number distribution vs. s (≡ (chord wise length measured from the leading edge) $/a$) for a uniform surface temperature.

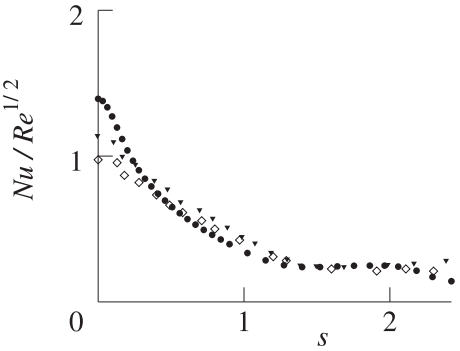

Figure 1: Local Nusselt number distribution. s: dimensionless arc length measured from the leading edge ($\beta = \pi$) based on a. •: current, $Re = 6000$, $Pr = 0.7$, $\epsilon_2 = -0.1$, $\epsilon_n = 0$ ($n \geq 3$), drag coefficient, $C_D = 0.375$ based on $\rho U_\infty^2 a$, ρ: density. ⋄: experimental [14], $Re = 4700$, based on a, no strong separation; ▼: experimental [14], $Re = 11200$, no strong separation. They are in good agreement each other

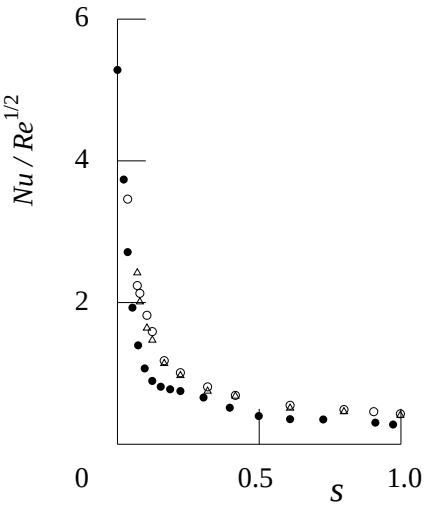

Figure 2: Nu-distribution. Experimental ones [7] correspond to NACA 65, 2-016 Airfoil, for which maximum height/half of the chord length ≈ 0.16. •: current, $b/a = 0.16$, $\epsilon_2 = -0.1$, $\epsilon_n = 0$ ($n \geq 3$), $Re = 5 \times 10^6$, $Pr = 0.7$; ○: experimental [7], $Re = 3.35 \times 10^6$ (air); △: experimental [7], $Re = 5.36 \times 10^6$. For an NACA airfoil, leading edge radius of curvature/a half chord length = 0.03408, whereas for the elliptic section the leading radius of curvature/$a = 0.0256$.
As far as symmetric streamline body is concerned, the effect of the difference between radii of curvature at the leading edge does not seem remarkable

3.3. Comparison of computed local Nusselt number distribution with experimental ones for Lockheed airfoil 12A

Figure 3 shows local Nusselt number distribution vs. dimensionless chord length measured from the leading stagnation point (based on the half chord length).

3.4. Comparison of local Nusselt number distribution for uniform heat flux with that on the ellipsoidal case (three dimensional axisymmetric case)

Figure 4 shows the distribution of a local Nusselt number, Nu_s, where reference length for Nu_s is local arc length measured from the leading edge point. Re_s is a local Reynolds number based on local arc length and local potential flow speed.

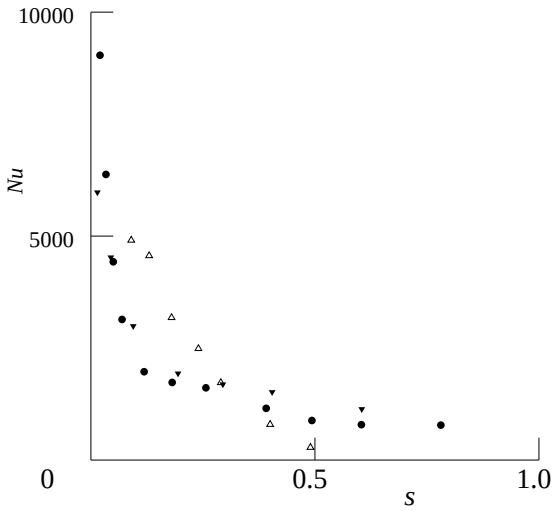

Figure 3: Nu-distribution. •: current, $Re = 5.1 \times 10^6$, $Pr = 0.7$, $\epsilon_2 = -0.1$, $\epsilon_n = 0$ ($n \geq 3$), $b/a = 0.145$, $C_D = 0.060$, $Nu_m = 1086$. △: experimental [2], on the upper wing; ▼: experimental [2], on the lower wing, $Re = 5.16 \times 10^6$

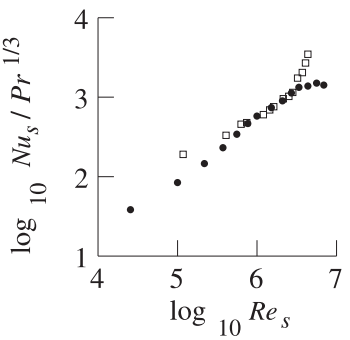

Figure 4: Nu_s-distribution, $b/a = 0.4$. •: current, $b/a = 0.4$, $\epsilon_2 = -0.1$, $\epsilon_n = 0$ ($n \geq 3$), $Re = 4 \times 10^6$, $Pr = 0.7$. □: experimental [8] (3-D ellipsoidal, stationary), $U_\infty = 78.2$ m/s, $a = 0.476$ m, ambient temp. $= -17.8$ (°C), ν (kinematic viscosity) $= 1.13 \times 10^{-5}$ m^{2}s^{-1}, $U_\infty a/\nu = 3.3 \times 10^6$.
Two-dimensional and three-dimensional heat transfer characteristics for uniform heat flux is quite similar in some interval of location (except the leading edge)

3.5. Comparison of a mean Nusselt number vs. a Reynolds number for various shapes (uniform surface temperature)

Figure 5 shows mean Nusselt number, Nu_m, vs. Reynolds number, Re. All experimental data are for air with uniform surface temperature, and reference length = one half of the body length in the flow direction unless otherwise stated.

4. Conclusions

At moderately high Reynolds number flows past an elliptic cylinder, heat transfer characteristics (independent of a Dirichlet type or a Neumann type) are widely obtained based on outer laminar potential flow with parametric variables. Computed results are in good agreement with traditional experimental data.

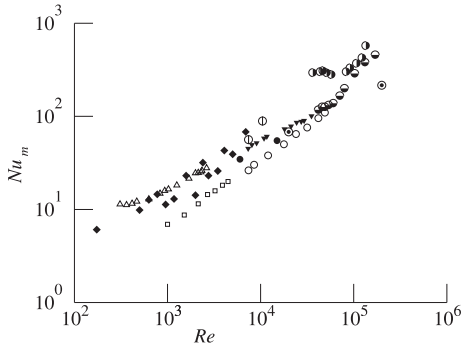

Figure 5: Nu_m vs. Re for various shapes. • current, $b/a = 1/2$, $\epsilon_2 = -0.1$, $\epsilon_n = 0$ $(n \geq 3)$, $Pr = 0.7$; ⊙: current, $b/a = 1/10$, $\epsilon_2 = -0.1$, $\epsilon_n = 0$ $(n \geq 3)$, $Pr = 0.7$; ⧫: experimental [4], from pin fin body array; ○: experimental [5], from finned cylinders, reference length = fin depth); △: experimental [16], elliptical tube rows; ▼: experimental [6], compact heat exchangers; ◑: experimental [15], compact heat exchangers of solar triangle; ◒: experimental [15], compact heat exchangers of plate fin surface; □: experimental [8], copper rectangular single fin; ⦶: experimental [9], diamond shaped array.
As far as mean Nusselt number is concerned, correlation seems good if the reference length is chosen as stated

References

[1] D. Akita, Y. Mochimaru. Numerical simulation of a flow past an elliptic cylinder at moderately high Reynolds numbers. *CMMPG*, **1** (2015), 1–7.

[2] H. J. Allen, B. C. Look. A method calculating heat transfer in the laminar flow region of bodies. NACA Report-No. 764, 1943, 177–182.

[3] M. T. Bhoite, S. Gavhane, M. Gore, S. Kanjvane. Numerical and experimental investigations on various fin configurations subjected to isoflux heating under the influence of convective cooling. *International Journal of Engineering Research and Applications*, **3** (2013), 15–18.

[4] K. T. Ciha. Pressure Loss through Multiple Rows of Various Short Pin Array Geometries & A Survey of Pressure Loss and Heat Transfer through Multiple Rows of Short Pin Arrays. University Turbine Systems Research (USTR) Industrial Fellowship Program 2014 Final Report, 2014.

[5] H. E. Ellerbrock, A. E. Biermann. Surface heat-transfer coefficients of finned cylinders. NACA Report No. 676, 1939, 651–664.

[6] R. Fehle, J. Klas, F. Mayinger. Investigation of local heat transfer in compact heat exchangers by holographic interferometry. *Experimental thermal and fluid science*, **1995** (1995), 181–191.

[7] C. W. Frick Jr., G. B. McCullough. Method for determing the rate of heat transfer from a wing or streamline body. NACA Report No. 830, 1945, 1–10.

[8] U. Glahn. Preliminary results of heat transfer from a stationary and rotating ellipsoidal spinner. NACA RM E53F02, 1953, 1–35.

[9] S. Hirasawa, A. Fujiwara, T. Kawanami, K. Shirai. Forced Convection Heat Transfer Coefficient and Pressure Drop of Diamond-Shaped Fin-Array. *Journal of Electronics Cooling and Thermal Control*, **4** (2014), 78–85.

[10] S. Kakaç, A. E. Bergles, F. Mayinger, H. Yüncü (eds) Heat transfer enhancement of heat exchangers, NATO ASI Ser. 355, 1999.

[11] S. Kakaç, R. K. Shah, A. E. Bergles (eds) Low Reynolds number flow heat exchangers, Hemisphere Pub., 1983.

[12] W. A. Khan, J. R. Culham, M. M. Yovanovich. Fluid Flow Around and Heat Transfer from Elliptical Cylinders: Analytical Approach. *Journal of Thermophysics and Heat Transfer*, **19** (2005), 178–185.

[13] S. A. Lawson, A. A. Thrift, K. A. Thole, A. Kohli. Heat transfer from multiple row arrays of low aspect ratio pin fins. *International Journal of Heat and Mass Transfer*, **54** (2011), 4099–4109.

[14] T. Ota, S. Aiba, T. Tsuruta, M. Kaga. Forced Convection Heat Transfer from an Elliptic Cylinder of Axis Ratio 1:2. *Bulletin of the JSME*, **26** (1983), 262–267.

[15] R. A. Riddell. Heat transfer and flow friction characteristics of a plate-fin type cross-flow heat exchanger with perforated fins. M.S., United States Naval Postgraduate School, 1966.

[16] S. M. Saboya. Transfer coefficients for plate fin and elliptical tube heat exchangers. COBEM'81, 1981, 153–162.

[17] L. Ventola, E. Chiavazzo, F. Calignano, D. Manfredi, P. Asinari. Heat Transfer Enhancement by Finned Heat Sinks with Micro-structured Roughness. *Journal of Physics: Conference Series*, **494** (2014), 1–9.

[18] L. W. Zhang, S. Balachandar. A Numerical Study of Flow and Heat Transfer in Compact Heat Exchangers. ACRCTR-103, 1996, 1–131.

Yoshihiro Mochimaru
Tokyo Institute of Technology
57-121, Yamaguchi, Tokorozawa
Saitama 359–1145, Japan
e-mail: ymochima-1947@cx.117.cx

Daisuke Akita
Dept. International
Development Engineering
Tokyo Institute of Technology
2-12-1 Ookayama, Meguro,
Tokyo 152-8550, Japan
e-mail: akita@ide.titech.ac.jp